inated by reducing the source bias voltage by an amount equal to the potential mismatch, i.e., the drift energy 8 eV. The dispersion when $V_0 = 18.4$ V (a drift is still evident for $V_0 = 19$ V) is shown by curve *b* in Fig. 3. I obtain a good fit to the data for $u_D = 0$, $T = 0.54$ eV, and $n_0 = n_B(0.7\ \text{kG})$ (charge collection yields $n_0 = 2.0 \times 10^6\ \text{cm}^{-3}$). In this case, no current is observed on the isolated tubes. The axial drift and the radial transport are reduced by adjusting the source parameters to conform with an allowable plasma equilibrium, in particular, with a plasma density below the Brillouin limit.

In summary, we have produced an ion plasma in which ion Langmuir waves are observed. The density constraint imposed by the Brillouin limit is experimentally verified. Near this limit, the plasma waves have dispersion properties similar to those of a weakly magnetized neutral plasma.

It is a pleasure to thank Professor J. Malmberg for suggesting a study of ion plasma waves and Dr. G. Morales for many useful discussions. The excellent technical support of G. Polidoro, G. Rosenthal, and R. Salazar is greatly appreciated. This research was supported by the National Science Foundation under Grant No. PHY-79-08480.

[1]R. C. Davidson, J. Plasma Phys. 6, 229 (1971).

[2]R. C. Davidson, *Theory of Nonneutral Plasmas* (Benjamin, Reading, Mass., 1974).

[3]R. C. Davidson and N. A. Krall, Phys. Fluids 13, 1543 (1970).

[4]A. W. Trivelpiece and R. W. Gould, J. Appl. Phys. 30, 1784 (1959).

[5]J. H. Malmberg and J. S. DeGrassie, Phys. Rev. Lett. 35, 577 (1975).

[6]A. Y. Wong, R. W. Motley, and N. D'Angelo, Phys. Rev. 133, A436 (1964).

[7]L. Brillouin, Phys. Rev. 67, 260 (1945).

[8]R. K. Feeney, W. E. Sayle, and J. W. Hooper, Rev. Sci. Instrum. 47, 964 (1976); S. Iizuka, K. Saeki, M. Sato, and Y. Hatta, Phys. Rev. Lett. 43, 1404 (1979).

[9]The mixture was 1:1 by weight. The cement is supplied by Alcoa (CA-25). It was chosen for its lack of alkalai impurities and its high-temperature capability.

[10]This is given by the second term in Eq. (2.6.21) in Ref. 2.

[11]When $\omega_p^2 = \Omega_0^2/2$, the rotational energy $mr^2\Omega_0^2/8$ exactly matches the radial-space-charge drop given by Eq. (1) and the plasma source must have an equipotential surface to avoid the sheared axial drifts.

[12]The derivation follows the calculation in Ref. 3 except their $k_\perp$ is replaced by the appropriate transverse derivative; see Ref. 4.

[13]B. D. Fried and S. Conte, *The Plasma Dispersion Function* (Academic, New York, 1961).

Visible Harmonic Emission as a Way of Measuring Profile Steepening

R. L. Carman, D. W. Forslund, and J. M. Kindel

Los Alamos Scientific Laboratory, University of California, Los Alamos, New Mexico 87545

(Received 15 September 1980)

First observed visible harmonics of CO_2-laser–irradiated plane and microballoon targets are reported. For intensities $> 5 \times 10^{14}$ W/cm^2, the harmonic production efficiency is constant over several visible harmonics with a cutoff at a high harmonic number. Two-dimensional particle simulations performed where there is a highly steepened density profile show a flat spectrum for high harmonics with a cutoff at the harmonic where the upper density shelf is underdense. Harmonics thus offer a means of measuring the upper density shelf and its dynamics.

PACS numbers: 52.25.Ps, 42.65.-k, 52.40.Jn, 78.40.-q

A number of theoretical and experimental papers address second-harmonic generation[1,2] in laser fusion experiments. Subharmonic and $\frac{3}{2}$-harmonic generation have also been discussed.[1,2] One group has reported seeing the third, fourth, fifth, sixth, tenth, and eleventh CO_2-harmonics in the backscattered beam direction.[1] They observed an approximately linear falloff in radiated harmonic with harmonic order, the ratio of *n*th to $(n+1)$th harmonic energies being ~6, for an incident CO_2-laser intensity $I_L > 10^{14}$ W/cm^2. Similar results have been observed at 1.06 μm for $I_L \sim 10^{16}$ W/cm^2 (same value of $I_L\lambda^2$).[2]

We report the observation of very-high-order CO_2-laser harmonics and a theoretical explanation of our experimental results. For the eight-beam CO_2-laser Helios system with $I_L \sim 3 \times 10^{16}$ W/cm^2, we observe harmonic light at as high as the 29th harmonic (365 nm) for plastic- and metal-coated glass microballoon (GMB) targets. In

plane target experiments performed at $I_L < 8 \times 10^{14}$ W/cm^2 at the Gemini laser system, we observe up to the twentieth harmonic emanating tangentially to the target, with the laser incident 15° off the target normal. In both sets of experiments, a new feature is observed, namely the harmonic generation efficiency is nearly constant in the observation direction from the sixteenth harmonic through the highest harmonic observed. Since the angular distribution of the harmonic light is currently not known experimentally, we are not able to quote a total efficiency with any confidence, but the harmonic brightness is at least 100-fold higher than plasma continuum light in the directions of observation [corresponding to $E_h \sim (10^{-4}-10^{-5})E_L$/harmonic if isotropically emitted].

The Gemini series of experiments were carried out with a single beam of 100 to 150 J on target in 1.0 to 1.2 ns [full width at half maximum (FWHM)]. The system operated on a single rotational line [$P(20)$] in the 10.6-μm vibrational band. The spectra were taken using two 20-cm–focal-length simple quartz-relay lenses operated at 1:1 magnification, a 1-m McPherson spectrograph ($F/8.7$), 2485 Kodak instrumentation film, and a 300-lines/mm grating blazed for 1 μm used in second order. Several plane targets (aluminum, titanium, iron, gold, copper, CH_2, and Teflon) were used. A typical spectrum obtained viewing the target at grazing incidence is shown in Fig. 1(a). After radiometric calibration of the spectrograph and correction for transmission variations, the harmonic production efficiency between the sixteenth CO_2-laser harmonic and the highest harmonic observed at a fixed exposure (typically the eighteenth and the twentieth) was determined to be the same to within 50%. For higher harmonics, the production efficiency dropped rapidly. The spectral linewidth was observed to be 100 ± 5 cm^{-1} FWHM for all harmonics, similar to the previous Nd:glass laser work.[2]

The Helios series of experiments were carried out with 750 to 950 J/beam in 600 to 750 ps (FWHM) pulses. By defocusing from the minimum spot size, the intensity in one beam could be varied from $\sim 10^{15}$ to 3×10^{16} W/cm^2. The oscillator normally operated on three to four rotational lines around $P(20)$ in the 10.6-μm band. The spectra were taken by use of two achromatic 25-cm–focal-length lenses at 1:1 magnification and the same spectrograph and film as in the Gemini series. Spherical targets, ranging in diameter from 250 to 1000 μm and fabricated from $(CH_2)_x$, copper, nickel, and gold, have been studied with no significant dependence noted for either target material or diameter. A typical tightly focused target spectrum in this series is shown in Fig. 1(b). The spectrograph observation direction is nominally 30° from the axis of one of the eight Helios beam lines. For this spectrum, we observe a similarly constant harmonic production efficiency out to at least the 25th harmonic, while the third-order spectra revealed the presence of at least the 29th harmonic. Further work is necessary to establish if the harmonic production efficiency is falling off above the 25th harmonic. This will require changing to re-

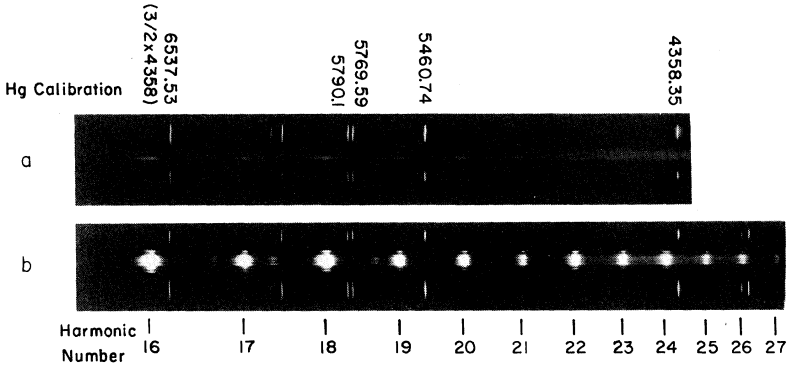

FIG. 1. Visible harmonic spectra obtained in CO_2-laser fusion experiments. (a) Gemini data for plane $(CH_2)_x$ target at $I_L \sim 5 \times 10^{14}$ W/cm^2 showing the sixteenth through the twentieth harmonics produced at the same conversion efficiency plus some hints of higher harmonics. (b) Helios data for spherical $(CH_2)_x$-coated BeCu target at $I_L \sim 3 \times 10^{16}$ W/cm^2 showing the sixteenth through 27th harmonics in second order as well as the 25th through the 29th harmonics in third order (the weaker satellites in the left-hand portion of the spectrum). The eighteenth and 27th harmonics overlap, as do the sixteenth and 24th harmonics.

flective optics in order to eliminate the effects of chromatic dispersion. Preliminary data suggest that the harmonic efficiency is constant to the 29th harmonic and possibly beyond.

Despite the change from single-rotational-line operation at Gemini to about four-rotational-line operation at Helios (with a total spread spectrally of <5.4 cm^{-1}), the harmonic linewidths for all Helios harmonics were still 100 ± 5 cm^{-1} FWHM. If this linewidth were to be attributed to a Doppler shift from a moving surface, velocities up to 2×10^7 cm/s could be inferred, but both inward and outward velocities must occur in order that the shift in the center frequency from the harmonic of CO_2-laser $P(20)$ (the dominant output) be <10 cm^{-1}, as observed.

Motivated by the above CO_2-laser target experiments, we have carried out two-dimensional particle simulations where pressure balance produces a highly steepened density profile. Typically, we observe a steepened density profile of $10n_c$ up to $100n_c$ and a lower density shelf of $0.1n_c$, where n_c is the critical density. The simulations are carried out with the electric field polarization in the plane of incidence.

The incident laser light undergoes a mode conversion in the steepened density profile to a surface plasma wave[3] resulting in a highly nonlinear form of resonant absorption. For this to occur, the incident light wave must be obliquely incident or be sufficiently focused that an electric field component along the density gradient exists. The plasma wave is highly nonlinear and, consequently, couples to the radiation field to cause emission at harmonics of the incident light wave. The level of harmonic emission is directly related to the amplitude of the plasma wave and the absorbed power. However, the primary dissipation of the plasma wave at high intensity is due to the wave accelerating a small fraction of the electrons in the steepened profile to high energies.[4]

In Fig. 2, we summarize results from a simulation in which a linearly polarized plane light wave is incident from the left at an angle of 23° to a sharp density profile, which is uniform in Y, the direction of periodicity. Pressure balance between the light and cold dense plasma produces an upper shelf of density

$$n_u \sim E_0^2/8\pi T_c \approx 45 n_c ,$$

where E_0 is the incident laser electric field and T_c is the cold background temperature, $I = 9 \times 10^{14}$ W/cm^2 and $T_c = 625$ eV. The self-consistent density profile and the corresponding plasma wave

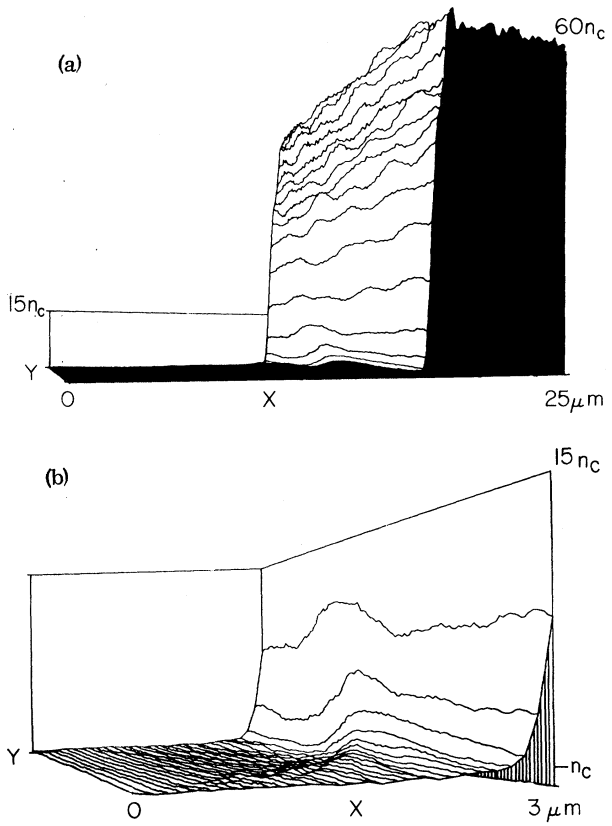

FIG. 2. Electron density profile for a wave simulation at $eE_0/m_e\omega_0 c = 0.3$, $T_e = 625$ eV, $M_i/m_e = 100$, $T_e/T_i = 10$, and 23° angle of incidence to the density gradient (a) vs x and y, where the self-consistent pressure balance density is $45n_c$, and (b) a blow-up plot of the base of the sharp-gradient region which isolates the plasma wave. Note contours in (a) and (b) are separated by only 0.1 μm.

density perturbation are shown in Fig. 2. Figures 2(a) and 2(b) are density plots versus x and y which vividly display the sharpness in the density profile, where the laser is incident from the left. Note that in Fig. 2(a) the density changes by $5n_c$ to $10n_c$ in 0.1 μm. Figure 2(b) is a magnified plot at the base of the sharp gradient region which isolates the plasma wave. Note the large amplitude nonsinusoidal surface perturbation traveling in the y direction. The low-density structure extending out from the plasma surface is formed by the ejected hot electrons from the plasma wave. The steepening of the plasma wave (harmonic generation) is closely associated with the ejection of these hot electrons.

In Figs. 3(a), 3(b), and 3(c), are plotted the calculated harmonic emission at three different intensities, respectively: 10^{14}, 4×10^{14}, and 9

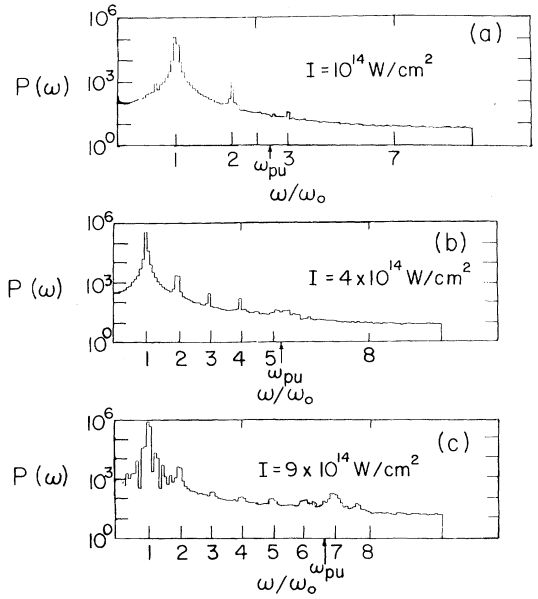

FIG. 3. Fourier power spectrum of the light leaving the left boundary of the simulation box for three laser intensities (a) 10^{14} W/cm^2 (i.e., $v_0/c = 0.1$), (b) 4×10^{14} W/cm^2, and (c) 9×10^{14} W/cm^2. Note the emission at harmonics of the laser. ω_{pu} corresponds to the plasma frequency at the upper shelf density.

$\times10^{14}$ W/cm^2. At 10^{14} W/cm^2, the steepened profile is $7n_c$, while at 4×10^{14} W/cm^2 it is $25n_c$. For the low-intensity case, the underdense shelf is at $0.25n_c$, while at the intermediate and high-intensity cases it is $0.1n_c$. The emission at $2\omega_0$ is different from emission at other harmonics and is typically at the 1% level. Emission at the third harmonic is down by another order of magnitude. For harmonics above the third we see an emission of about 10^{-4} of the fundamental. As the upper density increases with intensity, we see a flattening of the harmonic emission above $2\omega_0$ and a sharp cutoff at a high harmonic number. The cutoff corresponds approximately to the harmonic number to which the upper density shelf becomes underdense. The striking feature is the nearly constant efficiency of generation of the higher harmonic numbers until cutoff. A detailed theoretical analysis of the harmonic emission will be covered in a separate publication. However, the effect is clear from the fact that for $\omega > \omega_{pe}$, each harmonic is in resonance in the steep gradient. This should enhance the harmonic content of the plasma wave as well as the emitted harmonic light wave. Harmonic emission can develop for $\omega < \omega_{pe}$, but at a substantially lower efficiency. We have verified this scaling of the cutoff harmonic number by choosing a different simulation intensity and plasma temperature, which gives the same upper-shelf plasma density. We find that the cutoff harmonic number still lies at the plasma frequency of the upper shelf.

The simulation harmonic emission is in substantial agreement with the experimental results above, and is suggestive of how these results can be used to infer properties of the critical density. First, the cutoff in the harmonic spectrum immediately yields the density of the upper density shelf. The Gemini data at 8×10^{14} W/cm^2, which show a cutoff at the twentieth harmonic, would, therefore, suggest a steepened profile of 400 times the critical density. If we assume pressure balance based on a simple planar one-dimensional model, then we would infer a temperature for Gemini of less than 200 eV in the vicinity of the critical density. For Helios, the corresponding profile then must be at least $625n_c$, since a flattened spectrum out to at least the 25th harmonic is observed.

If the harmonic emission is temporally and spatially resolved, we can directly measure the position and velocity of the critical surface front. It is complementary to interferometry and, in particular, provides detailed information around the peak in the laser pulse—where collective processes would be expected to be strongest.

The authors are grateful to B. Bezzerides, C. Cranfill, R. Godwin, D. Giovanielli, K. Lee, and G. H. McCall for many useful discussions. We also wish to thank F. Wittman and N. Clabo for their able and helpful assistance in the performance of this experiment, as well as both technical staffs of the Gemini and Helios laser facilities. Finally, we thank E. Noveroske for his help with the digitizing and analysis of the spectra. This work was performed under the auspices of the U. S. Department of Energy.

[1]N. H. Burnett, H. A. Baldes, M. C. Richardson, and G. D. Enright, Appl. Phys. Lett. 31, 172 (1977), and references therein.

[2]E. A. McLean, J. A. Stamper, B. H. Ripin, H. R. Griem, J. McMahon, and S. E. Bodner, Appl. Phys. Lett. 31, 825 (1977), and references therein.

[3]J. M. Kindel, K. Lee, and E. L. Lindman, Phys. Rev. Lett. 34, 134 (1975), and references therein; M. M. Mueller, Phys. Rev. Lett. 30, 582 (1973); R. P. Godwin, Phys. Rev. Lett. 28, 85 (1972).

[4]B. Bezzerides, S. J. Gitomer, and D. W. Forslund, Phys. Rev. Lett. 44, 651 (1980); K. Estabrook and W. L. Kruer, Phys. Rev. Lett. 40, 42 (1978); D. W. Forslund, J. M. Kindel, and K. Lee, Phys. Rev. Lett. 39, 284 (1977).

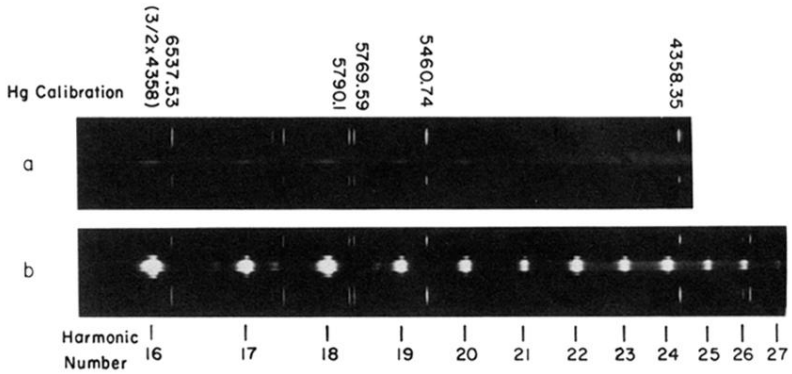

FIG. 1. Visible harmonic spectra obtained in CO_2-laser fusion experiments. (a) Gemini data for plane $(CH_2)_x$ target at $I_L \sim 5\times 10^{14}$ W/cm^2 showing the sixteenth through the twentieth harmonics produced at the same conversion efficiency plus some hints of higher harmonics. (b) Helios data for spherical $(CH_2)_x$-coated BeCu target at $I_L \sim 3\times 10^{16}$ W/cm^2 showing the sixteenth through 27th harmonics in second order as well as the 25th through the 29th harmonics in third order (the weaker satellites in the left-hand portion of the spectrum). The eighteenth and 27th harmonics overlap, as do the sixteenth and 24th harmonics.